





## Article

# Fast Pyrolysis of Tea Bush, Walnut Shell, and Pine Cone Mixture: Effect of Pyrolysis Parameters on Pyrolysis Crop Yields

Turgay Kar <sup>1</sup>, Ömer Kaygusuz <sup>2</sup>, Mükrimin Şevket Güney <sup>2</sup>, Erdem Cuce <sup>3,4</sup>, Sedat Keleş <sup>1</sup>, Saboor Shaik <sup>5</sup>, Abdulhameed Babatunde Owolabi <sup>6,7</sup>, Benyoh Emmanuel Kigha Nsafon <sup>8</sup>, Johnson Makinwa Ogunsua <sup>9</sup>, and Jeung-Soo Huh <sup>8,\*</sup>

- <sup>1</sup> Faculty of Science, Department of Chemistry, Karadeniz Technical University, 61080 Trabzon, Türkiye; karturgay1984@gmail.com (T.K.); sedat725@hotmail.com (S.K.)
- <sup>2</sup> Faculty of Engineering, Department of Mechanical Engineering, Giresun University, 28200 Giresun, Türkiye; omerkaygusuz061@gmail.com (Ö.K.); ms.guney@giresun.edu.tr (M.Ş.G.)
- <sup>3</sup> Department of Mechanical Engineering, Faculty of Engineering and Architecture, Zihni Derin Campus, Recep Tayyip Erdogan University, 53100 Rize, Türkiye; erdemcuce@gmail.com
- <sup>4</sup> School of Engineering and the Built Environment, Birmingham City University, Birmingham B4 7XG, UK
- <sup>5</sup> School of Mechanical Engineering, Vellore Institute of Technology (VIT), Vellore 632014, India; saboor.nitk@gmail.com
- <sup>6</sup> Regional Leading Research Center for Smart Energy System, Kyungpook National University, Sangju 37224, Republic of Korea; owolabiabdulhameed@gmail.com
- <sup>7</sup> Department of Convergence and Fusion System Engineering, Kyungpook National University, Sangju 37224, Republic of Korea
- <sup>8</sup> Department of Energy Convergence and Climate Change, Kyungpook National University, Buk-gu, Daegu 41566, Republic of Korea; luxnsafon@yahoo.ca
- <sup>9</sup> Postharvest Engineering Research Department, Nigerian Stored Products Research Institute, Ilorin 240003, Nigeria; jonehmak@gmail.com
- \* Correspondence: jshuh@knu.ac.kr



**Citation:** Kar, T.; Kaygusuz, Ö.; Güney, M.Ş.; Cuce, E.; Keleş, S.; Shaik, S.; Owolabi, A.B.; Nsafon, B.E.K.; Ogunsua, J.M.; Huh, J.-S. Fast Pyrolysis of Tea Bush, Walnut Shell, and Pine Cone Mixture: Effect of Pyrolysis Parameters on Pyrolysis Crop Yields. *Sustainability* **2023**, *15*, 13718. <https://doi.org/10.3390/su151813718>

Academic Editor: Domenico Licursi

Received: 31 July 2023

Revised: 24 August 2023

Accepted: 5 September 2023

Published: 14 September 2023



**Copyright:** © 2023 by the authors. Licensee MDPI, Basel, Switzerland. This article is an open access article distributed under the terms and conditions of the Creative Commons Attribution (CC BY) license (<https://creativecommons.org/licenses/by/4.0/>).

**Abstract:** Liquid products obtained by the fast pyrolysis process applied to biomass can be used as chemical raw materials and liquid fuels. In this study, tea bush, walnut shell, and pine cone samples selected as biomass samples were obtained from Trabzon and Rize provinces in the Eastern Black Sea Region and used. When considered in terms of our region, the available biomass waste samples are easy to access and have a high potential in quantity. To employ them in the experimental investigation, these biomass samples were first ground, sieved to a particle size of 1.0 mm, and mixed. A fast pyrolysis process was applied to this obtained biomass mixture in a fixed-bed pyrolysis reactor. The effects of temperature, heating rate, and nitrogen flow rate on the product yields of the fast pyrolysis technique used on the biomass mixture are examined. A constant particle size of 1.0 mm, temperatures of 300, 400, 500, 600, and 750 °C, heating rates of 100, 250, 400, and 600 °C.min<sup>-1</sup>, and flow rates of 50, 100, 200, and 300 cm<sup>3</sup>.min<sup>-1</sup> were used in tests on fast pyrolysis. The studies showed the 500 °C pyrolysis temperature, 100 °C min<sup>-1</sup> heating rate, and 50 cm<sup>3</sup>.min<sup>-1</sup> nitrogen flow rate gave the maximum liquid product yield. The liquid product generated under the most compelling circumstances is analyzed to determine moisture, calorific value, fixed carbon, ash, raw coke, and volatile matter. Additionally, the crude bio-oil heating value, measured at 5900 cal/g and produced under the most favorable pyrolysis circumstances, rose by around 40% compared to its starting material. The liquid product obtained from rapid pyrolysis experiments can be used as liquid fuel. The evaluation of the potential of chemical raw materials can be a subject of research in a different discipline since there are many chemical raw materials (glycerine, furfurals, cellulose and derivatives, carbonaceous materials, and so forth) in fast pyrolysis liquids.

**Keywords:** biomass; bio-oil; fast pyrolysis; walnut shell; pine cone; tea bush; heating rate

## 1. Introduction

In addition to the technological developments that arose from the increase in the population and facilitate people's lives, the increment in the energy consumption of the products has brought the search for new energy sources [1]. These increases in consumption have an adverse impact on some outputs, particularly the CO<sub>2</sub> emissions of primary energy sources often known as fossil fuels, like coal and oil. When these unfavorable effects have substantial side effects and repercussions that are difficult or expensive to reverse, the need for environmentally friendly, economically viable, and sustainable new energy sources has grown. The fact that energy consumption, which has a vital role in both social and economic terms, especially in modern industrial society, causes some environmental problems, especially the greenhouse effect, has increased the transfer to renewable and environmentally friendly alternative energy sources [2]. In this acceleration towards renewable energy sources, the increase in the cost of producing energy obtained by fossil sources is also of great importance. Energy expenditures, which have an essential place in our country's current account deficit, slow the pace of economic, cultural, technological, and social developments. When considering all these situations and developments, it is apparent that it is crucial to use the riches of our country, especially our renewable and domestic energy resources, consciously, with an ecological, environmentally friendly, and sustainable approach at the maximum level. Any non-fossil organic mass of biological origin that can renew itself in less than 20–30 years is referred to as biomass. In other words, biomass is the collective term for all biological elements that are not petrified and come from live or recently expired organisms. In this context, all organic materials of plant and animal origin, whose primary building blocks are carbohydrate molecules, are considered biomass energy sources. Biomass energy is the term used to describe the energy derived from these sources [3]. However, the biomass energy potential does not consider conventional forests, food, or agricultural products. In its natural state, biomass can be burned as fuel or transformed into various solid, gaseous, or liquid biofuels [4]. These fuels can be utilized for various industrial activities, including producing electricity, transportation, heating, and cooling. Therefore, essential solid biofuels, liquid biofuels, biogas, and municipal and industrial wastes are the typical classifications for biomass energy sources [5]. To understand the importance of biomass and biomass energy, it is necessary to look at the global warming and environmental pollution facing our world.

Average GHG emissions in the last ten years are the highest ever recorded, even though the increase in GHG emissions has been mitigated during the previous decade. Compared to the 2.6% growth each year between 2000 and 2009, the average yearly growth between 2010 and 2019 was 1.1%. The global decline in new coal capacity additions (especially in China), the continuous replacement of coal by gas in industrialized nations' power sectors, and the accelerating rate of renewable energy installations globally are all contributing factors to this decadal downturn [6,7]. The study of total world GHG emissions for 2021 is limited since estimates of land use, land-utilization modification, and forestry (LULUCF) are only currently available up to 2020. However, preliminary estimates of global GHG emissions for 2021, excluding LULUCF, are 52.8 GtCO<sub>2</sub>e, a slight rise over 2019. This indicates that total global GHG emissions in 2021 will be comparable to or potentially above the record 2019 levels. This supports past results showing that the COVID-19 pandemic reaction resulted in an exceptional but transient decrease in world emissions. Global GHG emissions diminished by 4.7% between 2019 and 2020. This fall gave rise to a significant 5.6% decrease in CO<sub>2</sub> emissions from industry and fossil fuels in 2020. Global coal emissions surpassed 2019 levels in 2021, although CO<sub>2</sub> emissions bounced back to 2019 levels. Between 2019 and 2021, fluorinated gas emissions increased while methane and nitrous oxide remained stable [8].

Regarding biomass production, Turkey has favorable sunlight, access to agricultural areas, water resources, and climatic conditions. Additionally, the country has a structure that may offer abundant resources for biomass energy. Although installed power has changed over time and Turkey's share of total installed power has increased, installed

power based on biomass and waste heat energy was only 2172 MW as of the end of June 2022 [9], and its share of total installed power was 2.14%. As a result, this potential can only be utilized partly effectively. The primary energy sources that come from biomass are heat and electricity. Even today, wood and other biomass wastes are used for cooking and heating, particularly in rural regions. However, the steam produced by biomass combustion boilers is utilized in industry for single or double heating [10].

Additionally, pressed cylindrical particles (pellets) made from wood sawdust have been burned in household stoves more and more recently for cooking or heating reasons [11]. Once more, electricity is generated, and the need for electricity is satisfied with less air pollution and more domestic resources by burning wood and coal in thermal power plants. Thus, it is feasible to generate power locally while utilizing less-polluting techniques by combining fossil fuel coal with renewable and cleaner biomass [12,13].

In contrast to combustion, pyrolysis occurs in the absence of oxygen, although partial combustion is used to generate the heat needed for this process to continue. By quickly heating the biomass at temperatures exceeding 300–400 °C, the biomass is converted into gas, liquid, and solid products [14]. As previously noted, pyrolysis entails the disintegration of big, complicated molecules into several smaller compounds. The item is divided into three primary categories:

- Liquid (water, tar, and heavier hydrocarbons);
- Solid (carbon-rich or primarily carbon-rich);
- Gases, such as H<sub>2</sub>, CO<sub>2</sub>, CO, C<sub>2</sub>H<sub>2</sub>, C<sub>2</sub>H<sub>4</sub>, C<sub>2</sub>H<sub>6</sub>.

Two crucial factors that determine the relative amounts of these products are the rate of heating and the maximum temperature that the biomass achieves. The volatile matter of the fuel should not be confused with the pyrolysis product. The pyrolysis temperature impacts the product's composition and yield [15]. Different product gases change at various temperatures during the pyrolysis of biomass. As a result, the emission rates for the various gas constituents vary greatly. The pyrolysis temperature also affects how much carbonized solid is generated [16,17]. Higher temperatures cause less char to form, while lower temperatures bring about more char. The temperature increase causes the organics to break down into smaller units. The biomass particle heating rate significantly influences the yield and content of the product. Slower heating results in more char, whereas rapid heating to moderate temperatures (400–600 °C) for quick pyrolysis yields greater condensing volatiles and, hence, more liquid output [18]. Debdoubi and colleagues observed a significant increase in liquid yield during Esparto's pyrolysis at 550 °C, with heating rates increasing from 50 °C.min<sup>-1</sup> to 250 °C.min<sup>-1</sup> [19]. However, heating rate and temperature alone do not define product yield and composition. Another crucial factor is the product's residence time in the reactor [20]. When volatiles are slowly or gradually removed from the reactor during slow heating, a secondary reaction occurs between the char particles and the volatiles, producing a secondary charred solid. To fulfill the needs of each final product, the pyrolysis device's operating settings are modified. The entraining gas flow rate is an essential factor for fast pyrolysis.

The pyrolysis vapors can be swiftly evacuated from the environment thanks to the fast flow rate of the entraining gas, preventing secondary reactions and increasing the yield of the liquid product. The environment's vapors are swiftly transported to the cooling system if the flow rate of the entraining gas is too high, making it difficult for the steam to condense. Several studies have been published in the literature to measure the entraining gas flow rate during rapid pyrolysis at various temperatures [21–26]. Turkey can be considered quite rich regarding the raw material waste resources used in this study. According to FAO 2022 data, Turkey ranks fourth in walnut production after China, the USA, and Iran, with its output approaching 300,000 tons [27]. In addition, when the current situation for the tea bush, which is another raw material used in this study, is evaluated, as of 2022, 791,287 decares [28] of tea area are pruned with the 1/7 pruning law every year, which constitutes a substantial potential in terms of biomass waste. Considering the pine cone, the third waste biomass used in this study, in Turkey, according to OGM (Turkey General

Directorate of Forestry) 2023 data, with the existence of approximately 11 million hectares of coniferous trees [29], cones provide an important biomass waste source. This investigation subjects these three distinct current waste biomasses to fast pyrolysis, and the quantities of liquid, solid, and gas generated are determined. The characteristics influencing product quantities are assessed, and the liquid product's energy content is compared to its raw material. Tea bushes, walnut shells, and pine cones are biomass raw materials used as waste in our country and are abundantly available. We think these materials, which are used directly as fuel, will be important sources of raw material for the fast pyrolysis of liquid fuel and for a biomass plant to be implemented in the future. This first-time, study examines the pyrolysis of these three biomass types together and the effects of pyrolysis parameters on product amounts. It will make essential contributions to the preliminary studies of the facilities to be established to evaluate their current potential.

## 2. Materials

Tea bush, walnut shell, and pine cone are utilized as raw materials in rapid pyrolysis studies. There are 830 thousand hectares of tea area in Turkey's Eastern Black Sea Region. These tea garden bushes, which are cut every year, are burned using traditional methods and used for heating. With around 80 million hectares, Turkey offers a diverse mountainous and ecogeographic landscape. In addition to this biological complexity, its forests are highly diverse in terms of species and composition. As a result, there are no barriers to the availability of raw material wastes employed in quick pyrolysis investigations.

### 2.1. Preparation of Biomass Samples Used as Raw Material

All biomass samples utilized are first cut into 1–2 cm spalls, and each biomass sample is ground in a mill. Afterward, the samples are passed through appropriate sieves to separate the ground samples into the predetermined particle size.

When agricultural products are placed in a particular environment, they exchange moisture with their environment. If the vapor pressure of the water in the product is greater than the partial vapor pressure of the water vapor in the ambient air, water vapor is released from the product into the environment. Conversely, water vapor transfers from the ambient air to the product. These moisture transitions continue until the vapor pressures of both environments equalize. When the equilibrium condition occurs, changes in the moisture value of the product cease. For this purpose, biomass sample mixtures were mixed in equal proportions, and spread in a thin layer on a flat, clean surface for ten days to equilibrate with the humidity in the laboratory environment.

### 2.2. Proximate Analysis of Biomass Samples

Analyses of moisture, calorific value, fixed carbon, ash, raw coke, and volatile matter were carried out on a biomass mixture of three distinct raw materials (tea bush, walnut shell, and pine cone).

#### 2.2.1. Determination of Moisture

The samples were kept in contact with air for ten days before the moisture content was determined. The moisture percentage was calculated by a predetermined 1 mm particle size sample of the biomass mixture. One gram samples of the tea bush, walnut shell, and pine cone were weighed at 0.1% sensitivity and maintained in an oven at  $103 \pm 2$  °C until they attained a consistent weight. The oven samples were cooled in a desiccator, weighed, and the moisture content was calculated, as shown below.

$$\text{Moisture (\%)}: [(w_1 - w_2)/w_1] \times 100$$

$w_1$ : Initial weight of the sample (g).

$w_2$ : Weighing of the sample after drying (g).

### 2.2.2. Determination of Volatile Matter

The biomass sample was heated in a platinum crucible for 10 min and then weighed after cooling in a desiccator. In this process, the remaining substance in the crucible is the volatile and dehumidified residue of the biomass sample, which is called raw coke.

Components other than raw coke are volatile and moisture components. The following equation substitutes moisture content values, calculating volatile matter (wt%) and determining the corresponding percentage. The following equation shows the ratio calculation by weight of the raw coke amount:

$$\text{Volatile substance amount (\%)} = 100 - (\text{raw coke (\%)} + \text{moisture (\%)})$$

$$\text{Raw coke amount (\%)} = [(w_1 - w_2)/w_0] \times 100$$

$w_1$ : The sum of the weights of the platinum crucible and the residue in it after heating (g)

$w_2$ : Weight of empty platinum crucible (tare) (g)

$w_0$ : Weight of the biomass sample initially placed in the platinum crucible (g).

### 2.2.3. Ash Content Determination

The sample taken from the biomass mixture was placed in a platinum crucible as a 1 g sample weighed with 0.1 mg precision and kept in an oven heated to 600 °C for three hours. Then, the samples kept in the desiccator were weighed, and the ash amounts were calculated as in below:

$$\text{Ash amount (\%)} = [(w_1 - w_2)/w_0] \times 100$$

$w_1$ : Sum of the platinum crucible and residual ash weight (g)

$w_2$ : Weight of empty platinum crucible (tare) (g)

$w_0$ : Weight of the biomass sample initially placed in the platinum crucible (g).

### 2.2.4. Determination of Fixed Carbon Amount

The following equation shows that the fixed carbon amounts are determined after calculating the biomass combination's moisture, ash, and volatile matter quantities:

$$\text{Fixed carbon (\%)} = 100 - (\text{ash} + \text{moisture} + \text{volatile matter})$$

### 2.2.5. Heating Value of Bio-Oil and Biomass Mixture

The heating values of bio-oil and the biomass mixture were measured in cal/g with the measurements made on the calorimeter device of IKA C 200.

## 2.3. Pyrolysis of Biomass Mixture

The pyrolysis studies were carried out in a 70 cm<sup>3</sup> fixed-bed tubular reactor built of stainless steel pipe and put in an insulated ceramic pipe. While Figure 1 shows the raw materials and mixtures used in fast pyrolysis experiments, Figure 2 depicts the fast pyrolysis reactor.

1. Nitrogen tube
2. Nitrogen flow line from tube to flow meter
3. Flow meter
4. Flow line of nitrogen gas from the flow meter to the reactor
5. Sample filling inlet
6. Temperature meter
7. Pyrolysis Reactor
8. Digital temperature and pressure gauge
9. Solid product discharge section
10. Pyrolysis vapors flow line
11. Liquid product collection unit



12. Cooler unit
13. Power supply
14. Coolant inlet connection
15. Coolant outlet connection



**Figure 1.** The appearance of biomass samples and combinations (1—mixed biomass samples 2—walnut shell 3—tea bush 4—pine cone).

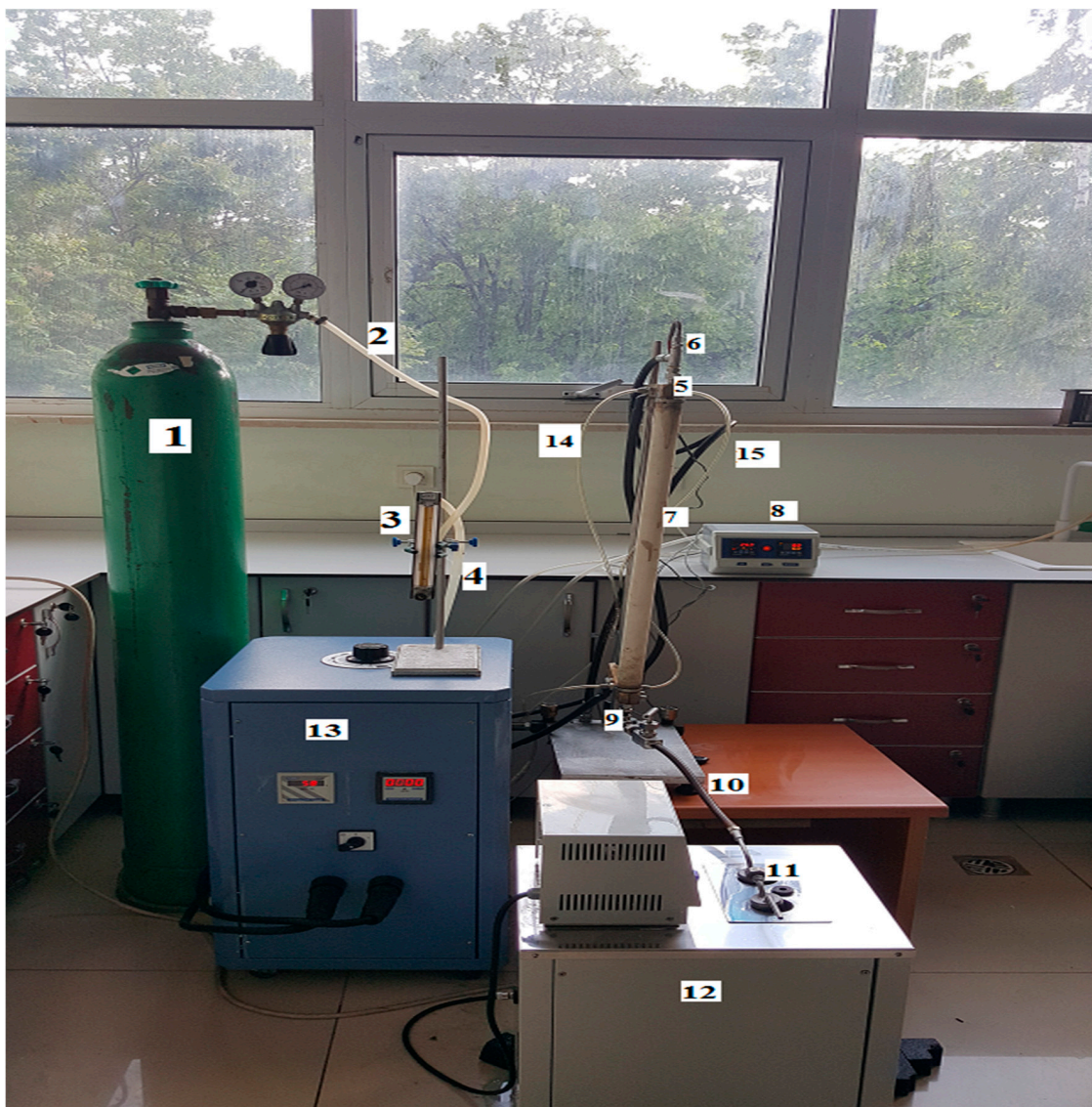


**Figure 2.** Shape and connected parts of the pyrolysis reactor.

Reactor: It has an instrument panel, a power system where temperature and heating rate can be controlled, and a thermocouple for temperature measurement. A flow meter coupled to a nitrogen cylinder regulated the nitrogen gas flow, which provided an inert atmosphere in the reactor and pushed the released gases from the reactor to the cooler. Liquid gaskets and clamps seal the nitrogen flow connections to the reactor. In addition, thin plastic hoses with constantly circulating tap water were wrapped around the reactor connections to minimize the damage to the reactor connections due to overheating. A Labo PL400-H22 refrigerated circulator device, which can cool down to  $-45\text{ }^{\circ}\text{C}$ , condensed the pyrolysis vapors. A collection vessel where the pyrolysis vapors were condensed was placed in a circulator containing an antifreeze-water mixture reduced to  $-45\text{ }^{\circ}\text{C}$ .

The pyrolysis vapors were connected to the inlet part of the collection vessel in the cooler utilizing a hose connected to the outlet of the reactor, and another hose was connected to the outlet part of the collection vessel to discharge non-condensable gases. The solid matter remaining in the reactor was weighed, and the amount of solid matter was determined as wt%. The sum of liquid, solid, and gaseous products was considered as one hundred percent and the amount of gaseous product was found by subtracting the total percent amount of liquid and solid products from the total percentage. The entraining nitrogen gas flow rates in the experiments were 50, 100, 200, and 300  $\text{cm}^3\cdot\text{min}^{-1}$ , the temperatures were 300, 400, 500, 600, and 750  $^{\circ}\text{C}$  and the heating rates were 100, 250, 400, and 600  $^{\circ}\text{C}\cdot\text{min}^{-1}$ . For current fast pyrolysis experiments, 1 g of samples were loaded into the reactor and arranged in a 1:1:1 ratio with constant particle size. In other words, tea bush, walnut shell, and pine cone, which constitute 1 g of biomass, were taken in equal proportions. In the experimental study, the studies were carried out to investigate three key parameters that influence the efficiency of the fast pyrolysis product. First, the impact of temperature on the efficiency of pyrolysis products was explored. Experiments were carried out at 300, 400, 500, 600, and 750  $^{\circ}\text{C}$  with 1 g of biomass mixture placed in a reactor of constant particle size (1 mm) (Figure 2).

Second, the influence of heating rate on the efficiency of pyrolysis products was explored. Again, a 1 g biomass mixture with a particle size of  $\leq 1$  mm was placed in the reactor, and tests were performed at heating rates of 100, 250, 400, and 600  $^{\circ}\text{C}\cdot\text{min}^{-1}$  and temperatures of 300, 400, 500, 600, and 750  $^{\circ}\text{C}$ . Third, the influence of nitrogen flow rate on the efficiency of pyrolysis products was explored. In the reactor, the  $\leq 1$  mm particle size biomass mixture was placed, and tests were performed at 300, 400, 500, 600, and 750  $^{\circ}\text{C}$  at 100, 250, 400, and 600  $^{\circ}\text{C}\cdot\text{min}^{-1}$  heating rates with a nitrogen flow of 50, 100, 200, and 300  $\text{cm}^3\cdot\text{min}^{-1}$ . The percentages of liquid, solid, gaseous, and pyrolysis conversions were computed as a consequence of the trials. All of the experiments in the research were repeated twice to obtain the findings.

### 3. Results and Discussion

The proximate analysis findings of the employed biomass mixture (pine cone, tea bush, walnut shell) are provided in this section. The findings of the experimental tests using the fast pyrolysis method are then presented in tables and graphics. The results for product efficiency are presented in graphs depicting the impacts of temperature, heating rate, and entraining nitrogen flow rate on product yields.

#### 3.1. Proximate Analysis Results Applied to the Biomass Sample Mixture

Table 1 shows the moisture, calorific value, fixed carbon, ash, raw coke, and volatile matter analytical findings of a biomass combination of three distinct raw materials (tea bush, walnut shell, and pine cone).

According to Table 1, as a result of the analyses applied to the biomass mixture used in this study, the amount of moisture is calculated as 13.04 wt%, the amount of volatile matter 61.26 wt%, the amount of ash 1.02 wt% and the amount of fixed carbon 24.68 wt%.

**Table 1.** Proximate analysis of the biomass mixture.

Analysis	Biomass Mixture
<sup>a</sup> Moisture (wt%)	13.04
<sup>b</sup> Volatile matter (wt%)	61.26
<sup>b</sup> Ash (wt%)	1.02
<sup>b</sup> Fixed carbon (wt%)	24.68
<sup>b</sup> Calorific value (MJ kg <sup>-1</sup> )	17.67

<sup>a</sup> as received. <sup>b</sup> weight percentage on dry basis.

The heating value of a raw material mixture of tea bush, walnut shell, and pine cone in equal quantities and subjected to fast pyrolysis is 17.67 MJ kg<sup>-1</sup>. The heating value of the raw bio-oil generated by fast pyrolysis is determined to be 24.66 MJ kg<sup>-1</sup> under the most efficient circumstances (50 cm<sup>3</sup>.min<sup>-1</sup> nitrogen flow rate, 100 °C.min<sup>-1</sup> heating rate, and 500 °C pyrolysis temperature).

### 3.2. Experimental Results from Fast Pyrolysis

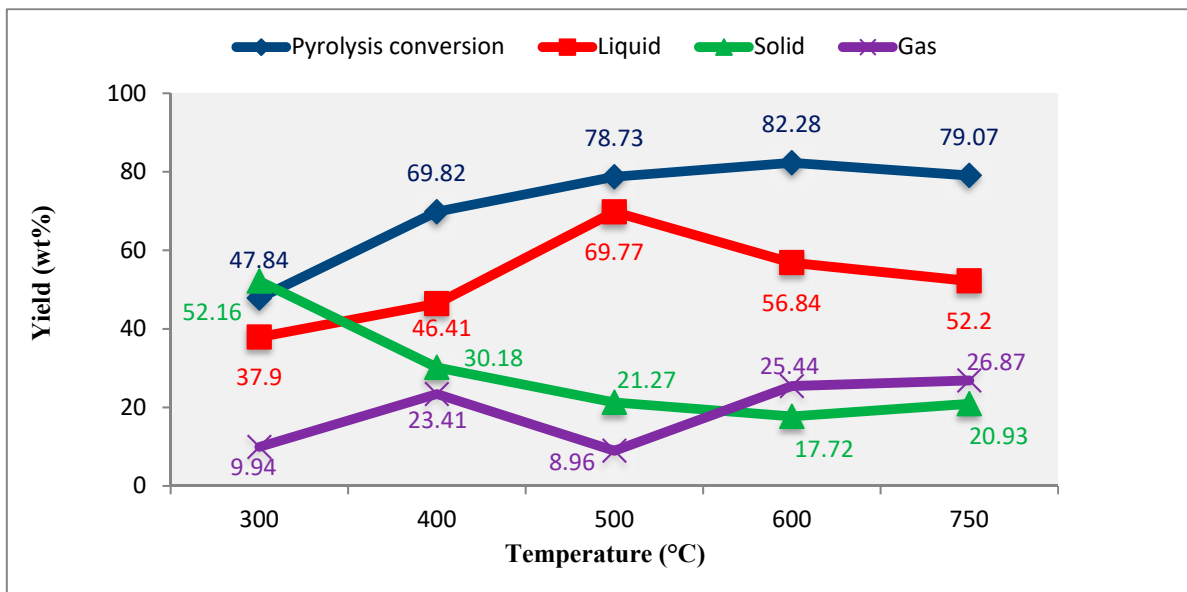
Fast pyrolysis experiments were prepared by weighing fixed particle size (1 mm) pine cones, tea bushes, and walnut shells at a ratio of 1:1:1, respectively, to form a mixture of 1 g. The experiments were performed by applying fast pyrolysis with entraining nitrogen flow rates at 50, 100, 200, and 300 cm<sup>3</sup>.min<sup>-1</sup>, temperatures at 300, 400, 500, 600, and 750 °C and heating rates of 100, 250, 400, and 600 °C.min<sup>-1</sup>.

### 3.3. Effect of Temperature on Pyrolysis Product Yields

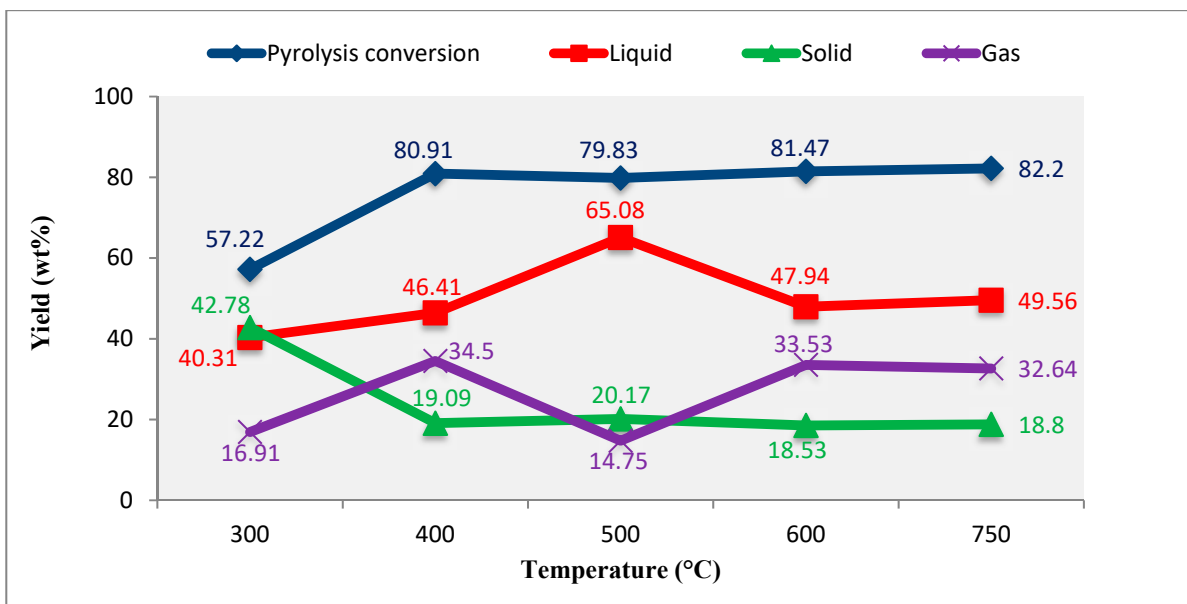
The temperature parameter used in the pyrolysis experiments of biomass significantly affects the yield and amount of the product formed as a result of pyrolysis. The bio-oil yields typically reach their highest concentrations between 400 and 550 °C and then start to fall as the heating process continues. The dominating secondary cracking reactions cause the bio-oil and char products to turn into gas at temperatures greater than 600 °C [30]. The bio-oil polar, aliphatic, and aromatic fractions are enhanced by raising the temperature from 300 to 500 °C to 600 to 800 °C [31]. The decarboxylation and dehydration processes at temperatures above 700 °C often increase the carbon content of bio-oils in the form of polycyclic aromatic hydrocarbons like pyrene and phenanthrene. Considering the literature mentioned earlier, the temperatures selected in this study are also within the temperature range used for fast pyrolysis. Increasing the pyrolysis temperature generally increases gas product production while decreasing solid product yield. While the liquid product efficiency increases at medium temperatures (400–500 °C), it declines as the temperature rises due to secondary processes that favor vapor breakdown [32]. The figures show the influence of pyrolysis temperature on product efficiency at dissimilar heating rates of the biomass combination employed at 300, 400, 500, 600, and 750 °C, as well as at 50 cm<sup>3</sup>.min<sup>-1</sup>, where the maximum liquid production is obtained.

Figure 3 shows the maximum liquid yield is obtained at 500 °C, with a value of 69.77 wt%. Though the liquid product changes with the heating rate, it is noted that the maximum liquid product efficiency is achieved at 500 °C in Figures 3–6. The maximum value is shown in Figure 3, where the greatest liquid product is acquired at a heating rate of 100 °C.min<sup>-1</sup>. The pyrolysis conversion in the experiment performed under these conditions is 78.73 wt%. The highest pyrolysis conversion percentage is 82.74 wt%. Figures 5 and 6 show pyrolysis conversion increases with temperature, attributed to increased liquid product yield up to 500 °C and gaseous product yield after 500 °C. This variability in pyrolysis product efficiency is consistent with the literature [33]. The efficiency of the liquid product is similarly poor at low temperatures, as shown in Figures 3–6.





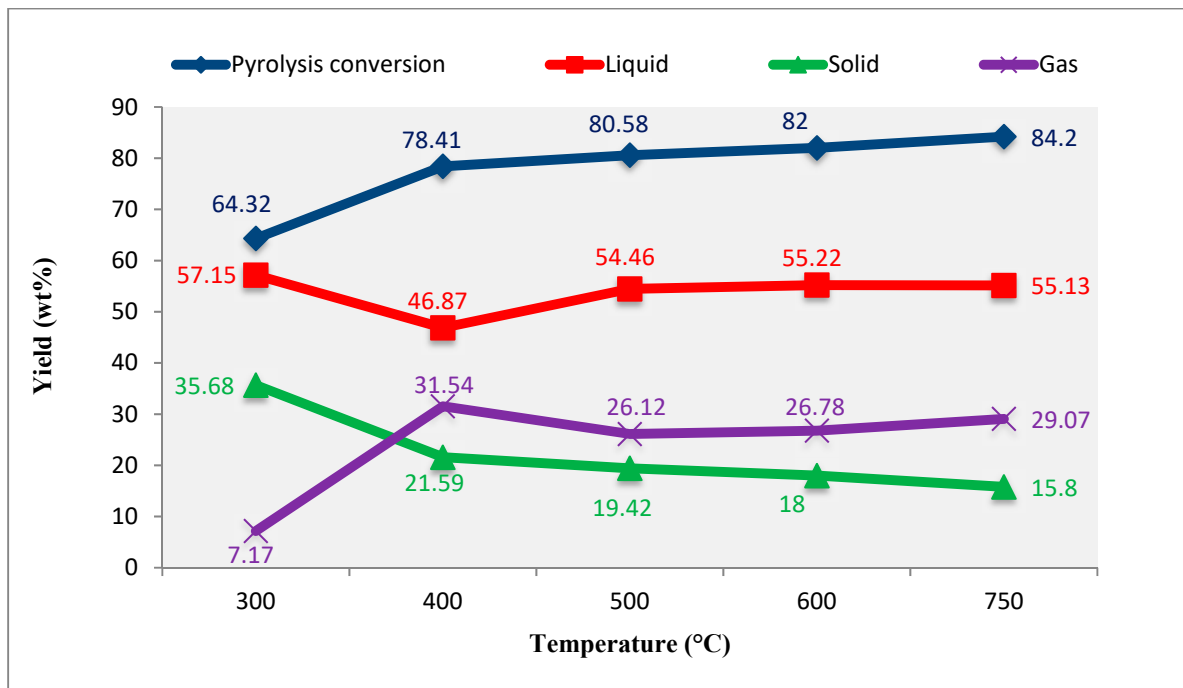
**Figure 3.** The effect of pyrolysis temperature on the product yield of  $50 \text{ cm}^3 \cdot \text{min}^{-1}$  nitrogen flow rate and  $100 \text{ }^\circ\text{C} \cdot \text{min}^{-1}$  heating rate on biomass mixture pyrolysis.



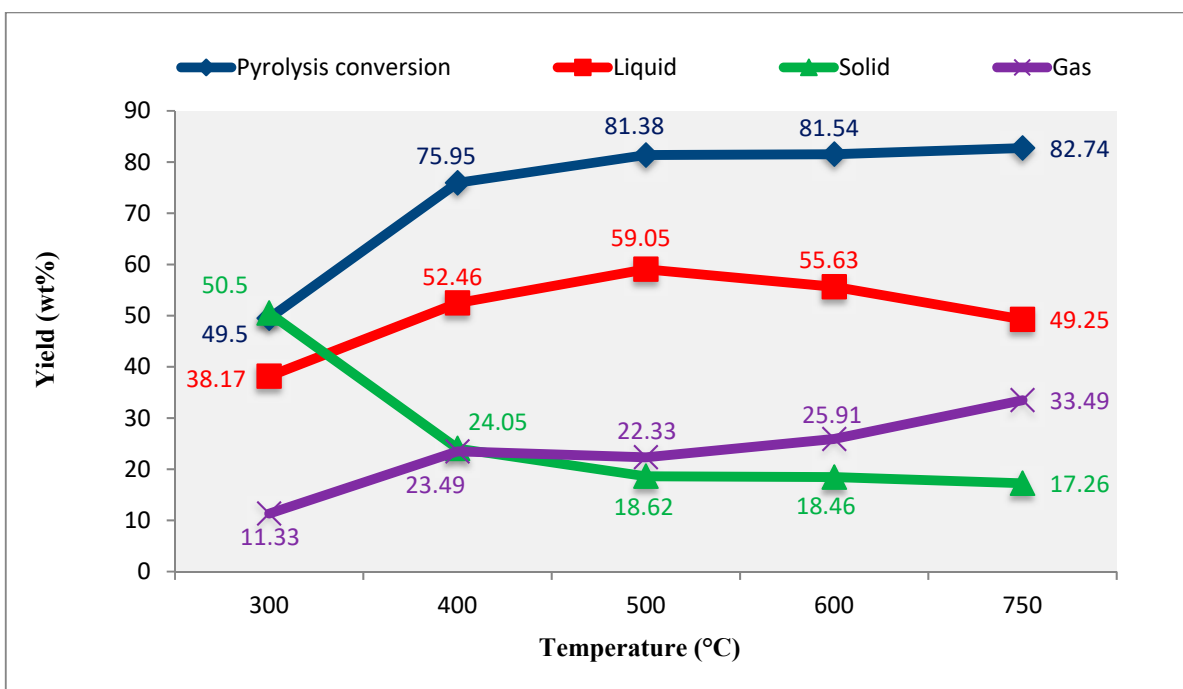
**Figure 4.** The effect of pyrolysis temperature on the product yield of  $50 \text{ cm}^3 \cdot \text{min}^{-1}$  nitrogen flow rate and  $250 \text{ }^\circ\text{C} \cdot \text{min}^{-1}$  heating rate on biomass mixture pyrolysis.

Figure 3 shows the lowest liquid product yield at  $100 \text{ }^\circ\text{C} \cdot \text{min}^{-1}$  and a pyrolysis temperature of  $300 \text{ }^\circ\text{C}$ . Figures 3–6 indicate decreased liquid product efficiency at temperatures above  $500 \text{ }^\circ\text{C}$  due to increased gas product efficiency. Again, when the graphs in Figures 3–6 are examined, it is observed that the solid product productivity decreases with the increase in temperature. Figure 4 demonstrates the minimum solid product at  $300 \text{ }^\circ\text{C}$  and  $400 \text{ }^\circ\text{C} \cdot \text{min}^{-1}$ . The maximum solid product yield is obtained at  $600 \text{ }^\circ\text{C} \cdot \text{min}^{-1}$  at  $300 \text{ }^\circ\text{C}$ . The efficiency of gas products rises with temperature, although the lowest values are obtained at  $500 \text{ }^\circ\text{C}$ . Temperature is responsible for the abrupt rise in liquid product efficiency. Figure 6 shows the maximum gas product yield at  $750 \text{ }^\circ\text{C}$  and a  $600 \text{ }^\circ\text{C} \cdot \text{min}^{-1}$  heating rate, while the minimum yield is at  $500 \text{ }^\circ\text{C}$  with a  $100 \text{ }^\circ\text{C} \cdot \text{min}^{-1}$  heating rate. In Figure 3, a temporary decrease in gas product yield was observed due to the sharp increase in liquid product yield when the temperature increased from  $400 \text{ }^\circ\text{C}$  to  $500 \text{ }^\circ\text{C}$ . Here, it is

thought that the sharp increase in the liquid product is due to the increase in the amount of condensable gases condensed in the cooler. When it increased from 500 °C to 600 °C, as expected, there was a decrease in the liquid product yield in parallel with the increase in gas product yield. Similar reasons can explain this imbalance in Figure 4. In addition, the decrease in solid and gas product yields approximately corresponds to the increase in liquid product yield when it is increased from 400 °C to 500 °C.



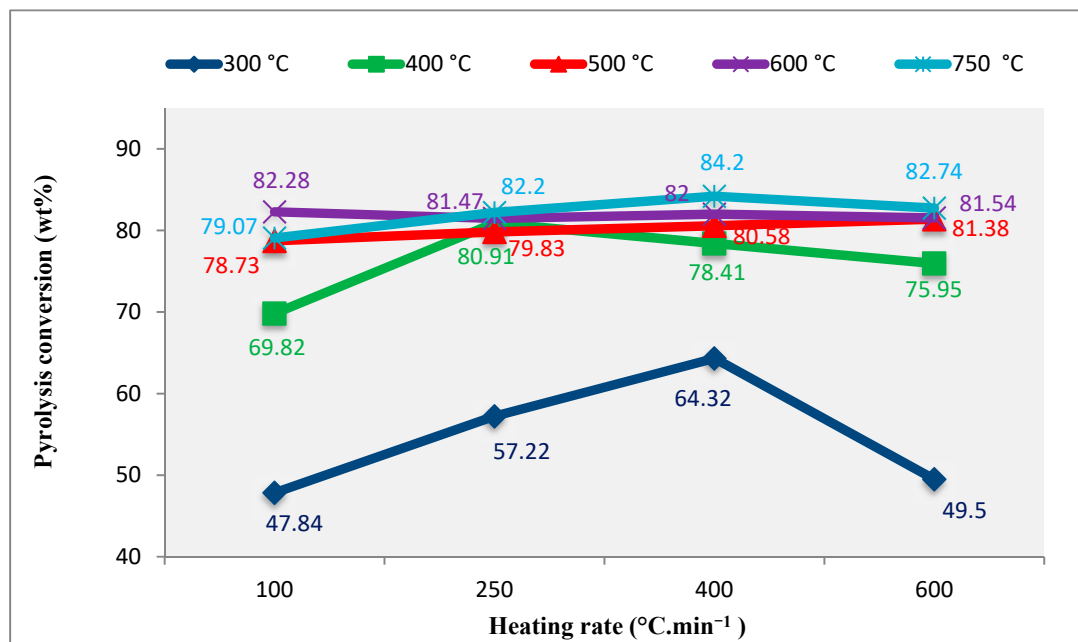
**Figure 5.** The effect of pyrolysis temperature on the product yield of 50 cm<sup>3</sup>.min<sup>-1</sup> nitrogen flow rate and 400 °C.min<sup>-1</sup> heating rate on biomass mixture pyrolysis.



**Figure 6.** The effect of pyrolysis temperature on the product yield of 50 cm<sup>3</sup>.min<sup>-1</sup> nitrogen flow rate and 600 °C.min<sup>-1</sup> heating rate on biomass mixture pyrolysis.

### 3.4. The Effect of Heating Rate on the Yields of Pyrolysis Products

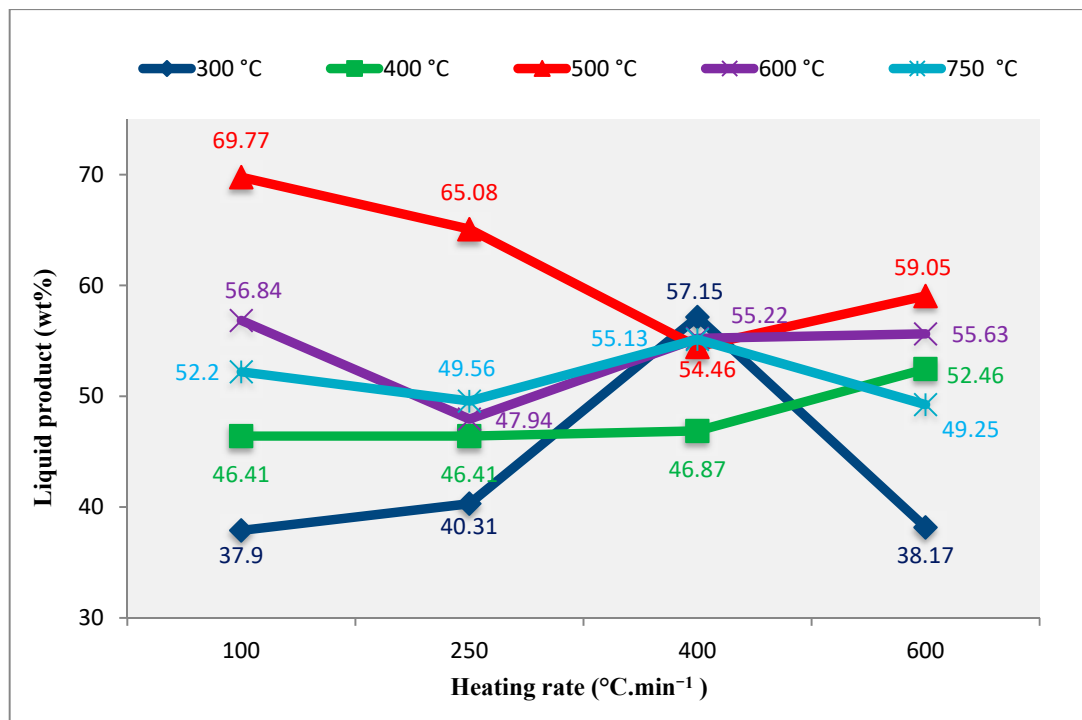
The heating rate is a critical characteristic that determines the type of biomass pyrolysis, which includes flash, rapid, and slow pyrolysis. Fast heating rates promote fast fragmentation of the biomass, resulting in more gases and less char. Because of the reduction in mass and heat transfer constraints and the short time available for secondary reactions, bio-oil production is also increased at high heating rates [34]. The heating rates selected in this study were determined by considering the literature [18,35–37]. The effect of different heating rates on pyrolysis conversion, liquid product yield, solid product yield, and gas product efficiency at a nitrogen flow rate of  $50 \text{ cm}^3 \cdot \text{min}^{-1}$ , where the maximum liquid product yield is obtained, is shown in Figures 7–10.



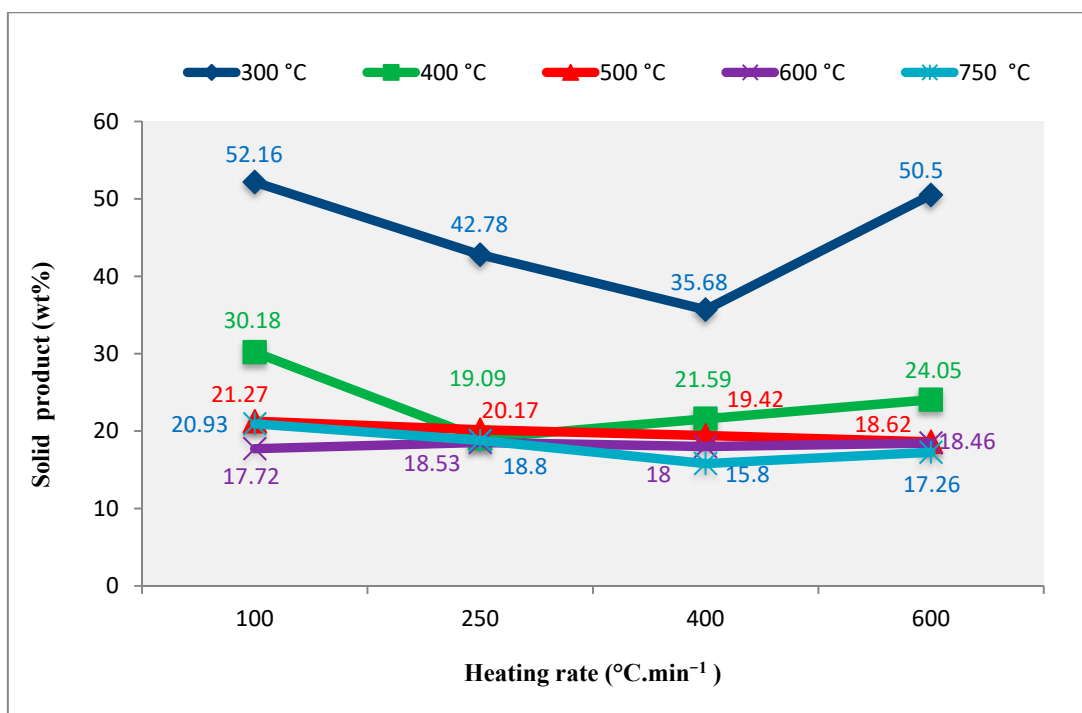
**Figure 7.** The effect of heating rate on pyrolysis conversion at different temperatures from the biomass mixture fast pyrolysis at a constant nitrogen flow rate ( $50 \text{ cm}^3 \cdot \text{min}^{-1}$ ).

Figure 7 shows that this conversion value of 84.2 wt%, when maximal pyrolysis conversion efficiency occurs, is obtained at  $400 \text{ }^{\circ}\text{C} \cdot \text{min}^{-1}$ . Pyrolysis conversion efficiencies increase with heating rate from  $100 \text{ }^{\circ}\text{C} \cdot \text{min}^{-1}$  to  $400 \text{ }^{\circ}\text{C} \cdot \text{min}^{-1}$ , while significantly reduced at  $600 \text{ }^{\circ}\text{C} \cdot \text{min}^{-1}$ . In experiments exploring the effect of heating rate on product yields, coking at a low temperature and a fast heating rate boosted solid product efficiency while decreasing liquid and gas product yields. This result is consistent with the findings of the literature [38]. The optimal heating rate for the liquid yield has been established to be  $100 \text{ }^{\circ}\text{C} \cdot \text{min}^{-1}$ . Since the sum of liquid and gaseous products do not alter much in pyrolysis conversion efficiencies at  $500 \text{ }^{\circ}\text{C}$ , no crucial measurable change is noticed in these conversion efficiencies when the heating rate is varied from  $100 \text{ }^{\circ}\text{C} \cdot \text{min}^{-1}$  to  $600 \text{ }^{\circ}\text{C} \cdot \text{min}^{-1}$ . Figure 8 indicates the greatest liquid product at  $500 \text{ }^{\circ}\text{C}$  and  $100 \text{ }^{\circ}\text{C} \cdot \text{min}^{-1}$ . At  $300 \text{ }^{\circ}\text{C}$  with a nitrogen flow rate of  $100 \text{ }^{\circ}\text{C} \cdot \text{min}^{-1}$ , the lowest value is 37.90 wt%. The rise in gas product yield is assumed to decrease liquid product yield at  $500 \text{ }^{\circ}\text{C}$  and  $400 \text{ }^{\circ}\text{C} \cdot \text{min}^{-1}$ . Additionally, it is noted that at high pyrolysis temperatures, the liquid product values at  $400 \text{ }^{\circ}\text{C} \cdot \text{min}^{-1}$  are relatively near to one another. Figure 9 represents the relationship between heating rate and solid product. The maximum solid product efficiency is found at  $300 \text{ }^{\circ}\text{C}$  and  $100 \text{ }^{\circ}\text{C} \cdot \text{min}^{-1}$ , while the minimum solid product efficiency is at  $750 \text{ }^{\circ}\text{C}$  and  $400 \text{ }^{\circ}\text{C} \cdot \text{min}^{-1}$ . Higher temperatures improve the production of liquid and gaseous products while decreasing the efficiency of solid products. Additionally, the solid product yield increases at heating rates of  $300 \text{ }^{\circ}\text{C} \cdot \text{min}^{-1}$  and  $600 \text{ }^{\circ}\text{C} \cdot \text{min}^{-1}$ ; this is because the solids agglomerate due to the high heating rate's impact on the biomass mixture in the reactor.

Figure 10 demonstrates the relationship between heating rate and gas product yield, with the maximum gas product efficiency occurring at  $250\text{ }^{\circ}\text{C}\cdot\text{min}^{-1}$  and  $400\text{ }^{\circ}\text{C}$ . At a heating rate of  $100\text{ }^{\circ}\text{C}\cdot\text{min}^{-1}$  and  $500\text{ }^{\circ}\text{C}$ , the lowest value is  $8.96\text{ wt}\%$ . The lowest gas product efficiency value of  $8.96\text{ wt}\%$  is observed when the liquid product is the maximum.



**Figure 8.** The effect of heating rate on the liquid product at different temperatures from the biomass mixture fast pyrolysis at a constant nitrogen flow rate ( $50\text{ cm}^3\cdot\text{min}^{-1}$ ).



**Figure 9.** The effect of heating rate on the solid product at different temperatures from biomass mixture pyrolysis at a constant nitrogen flow rate ( $50\text{ cm}^3\cdot\text{min}^{-1}$ ).



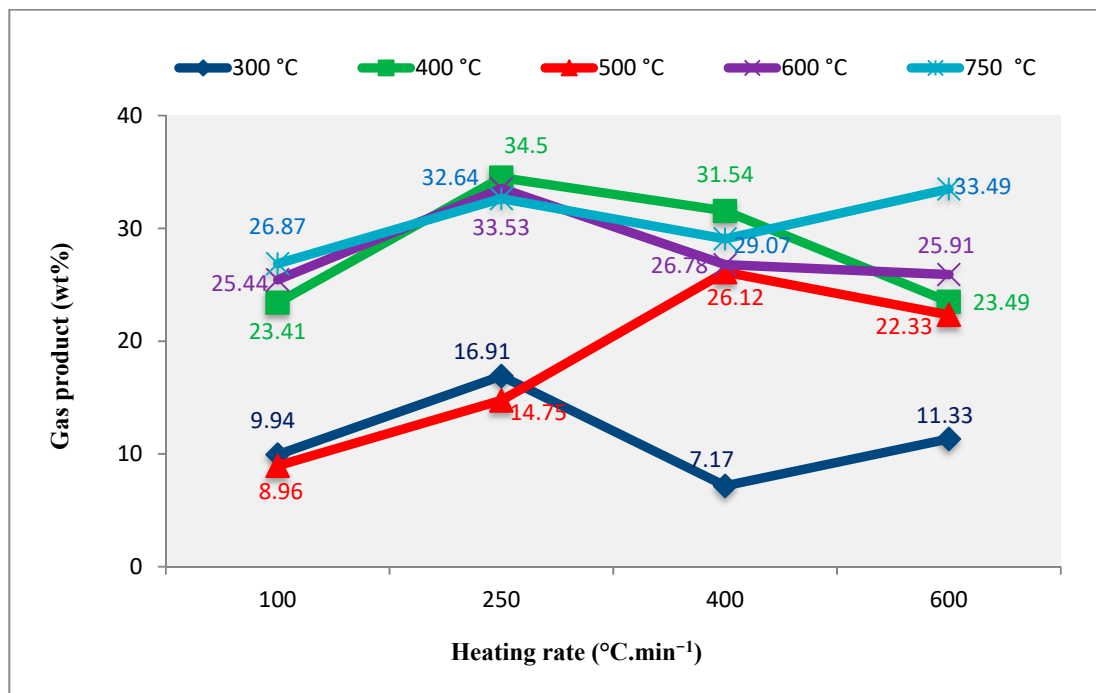


**Figure 10.** The effect of heating rate on the gas product at different temperatures from biomass mixture pyrolysis at a constant nitrogen flow rate (50 cm<sup>3</sup>.min<sup>-1</sup>).

### 3.5. Nitrogen Flow Rate Influence on Pyrolysis Product Yields

One of this study’s characteristics is the nitrogen flow velocity at a heating temperature 100 °C.min<sup>-1</sup> at distinct fast pyrolysis temperatures. Using the graphic data in Figures 11–15, the impacts of pyrolysis conversion, liquid efficiency, solid efficiency, and gas efficiency are assessed.

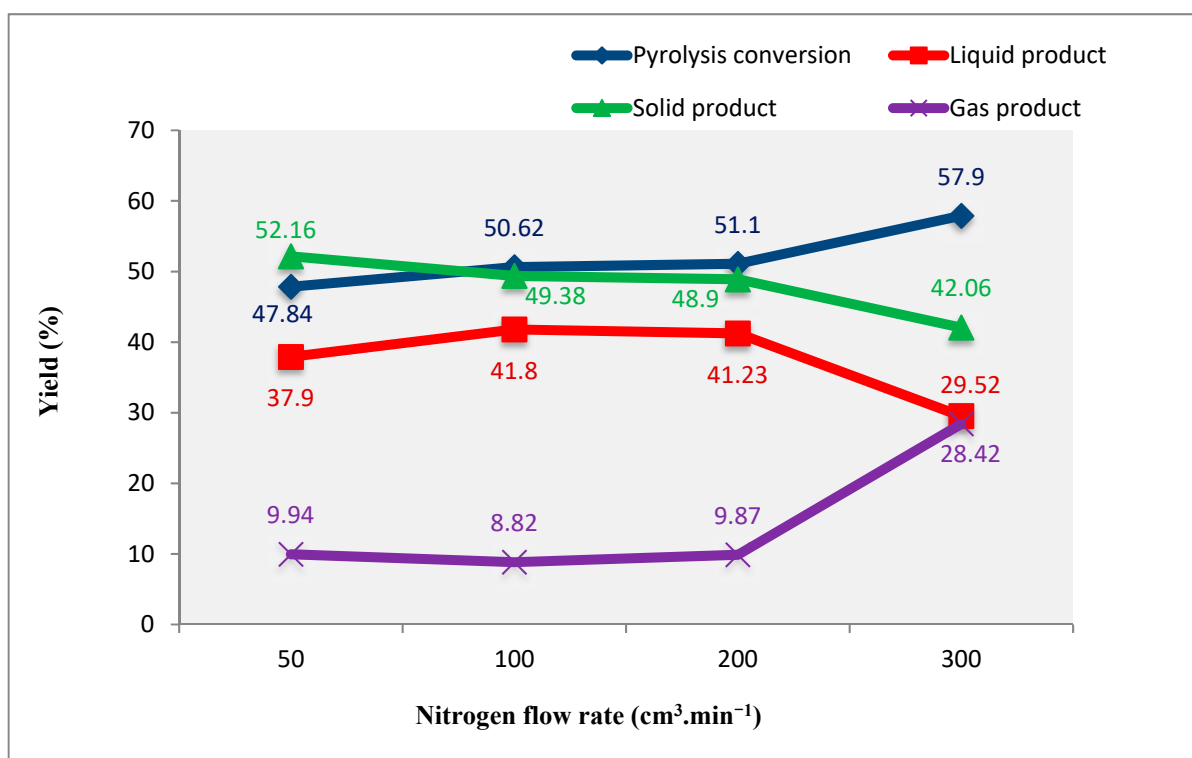


**Figure 11.** The impact of nitrogen flow rate on product efficiency at 300 °C and 100 °C.min<sup>-1</sup>.

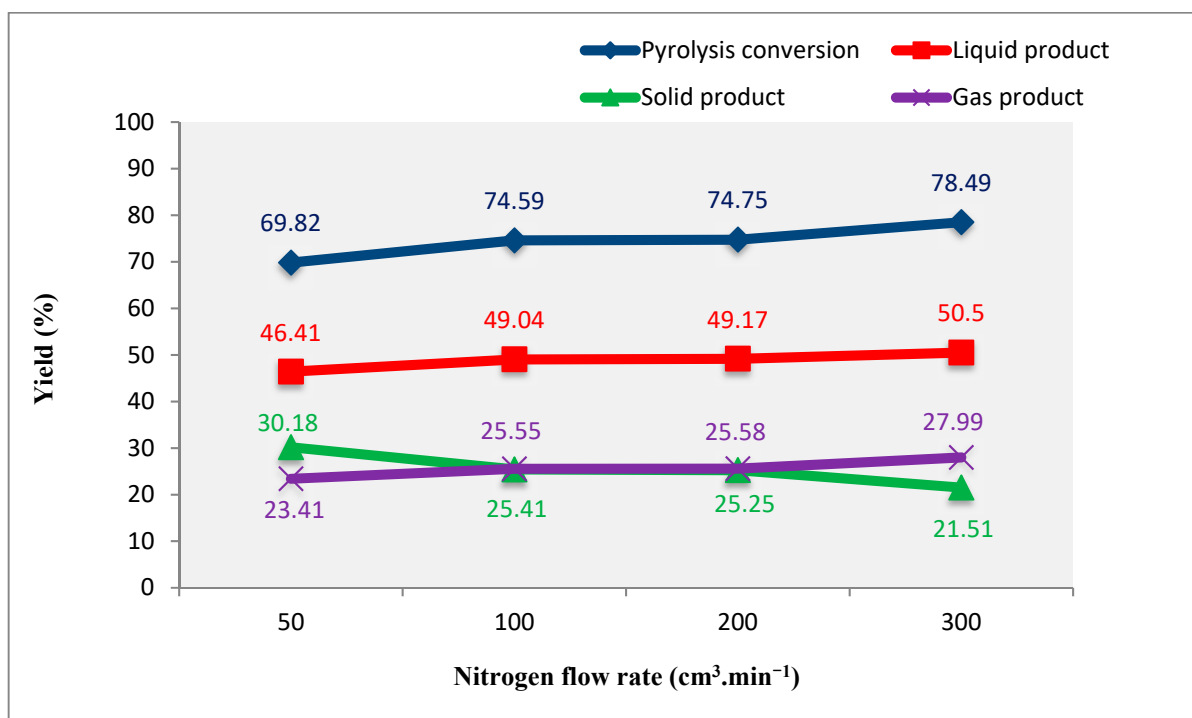


Figure 12. The impact of nitrogen flow rate on product yields at 400 °C and 100 °C.min<sup>-1</sup>.

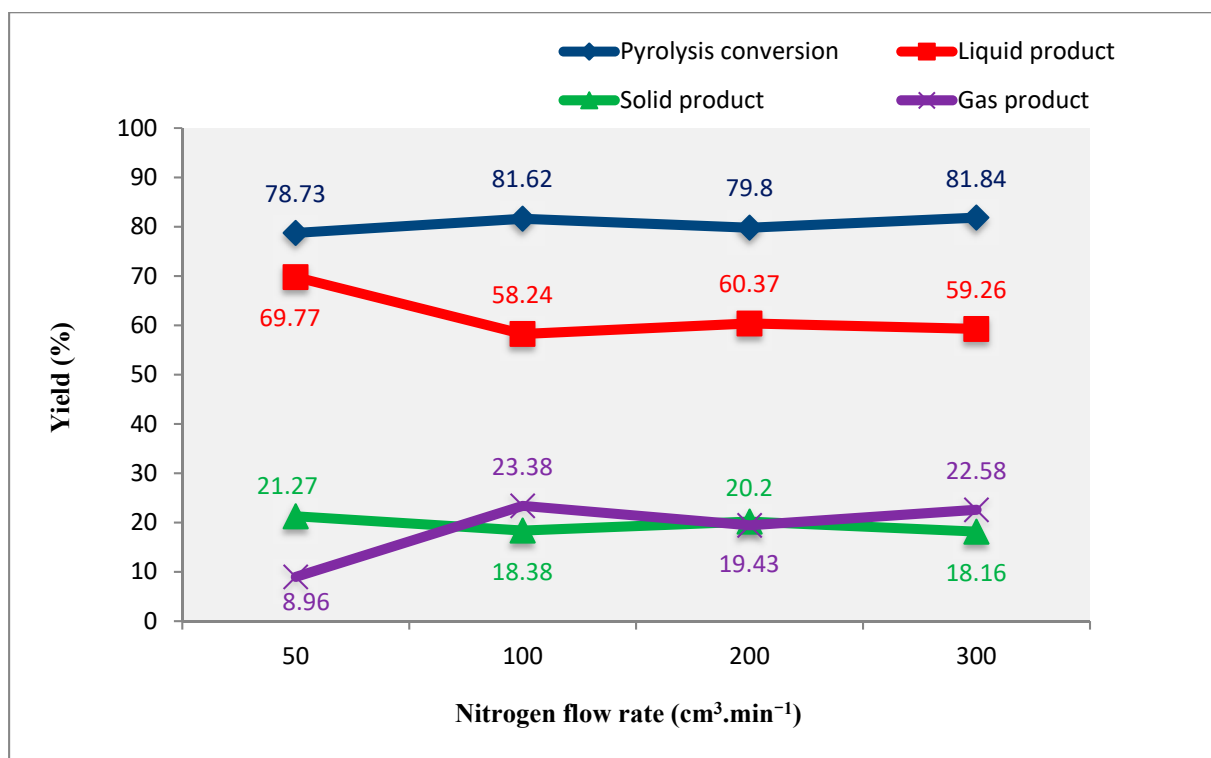
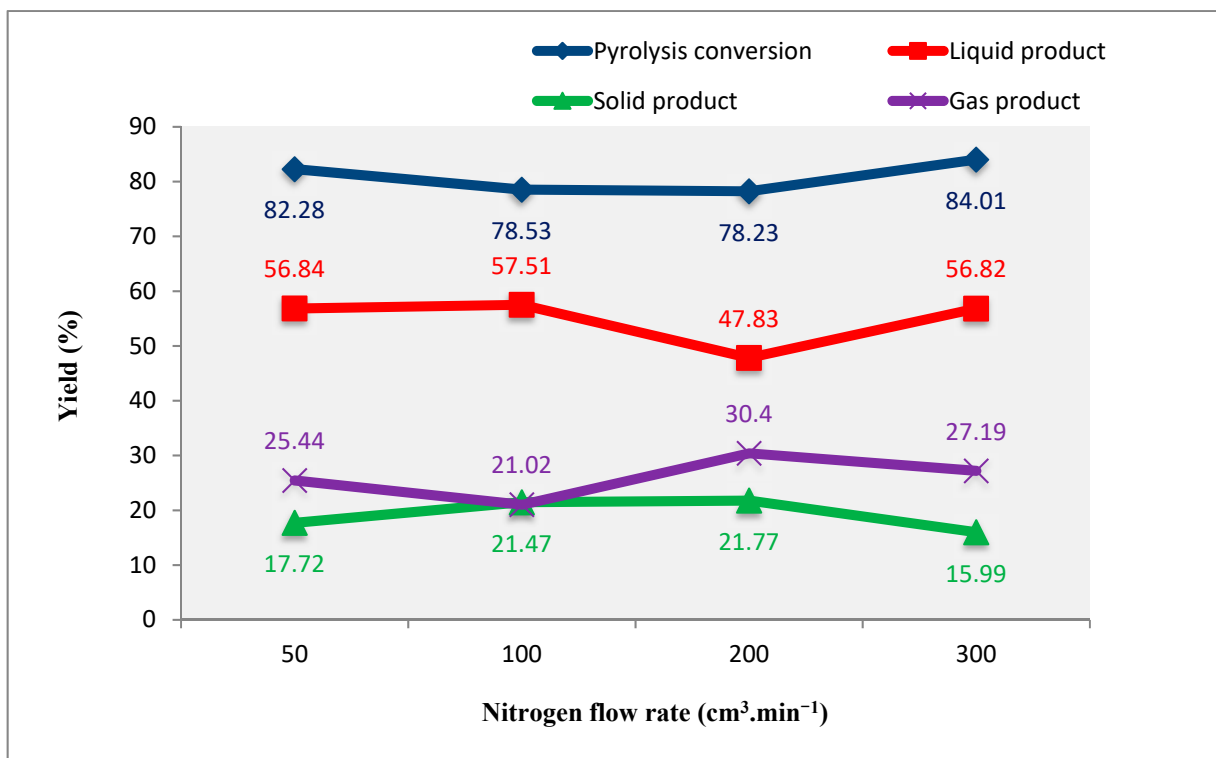
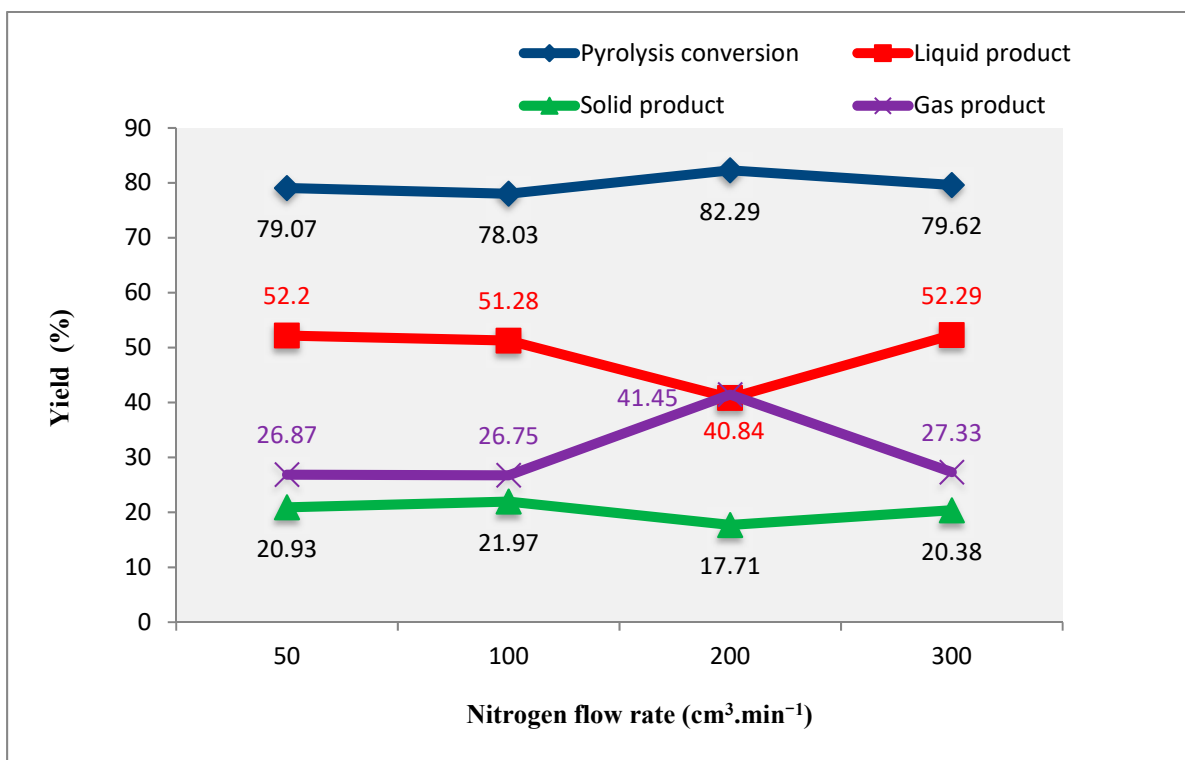


Figure 13. The impact of nitrogen flow rate on product efficiency at 500 °C and 100 °C.min<sup>-1</sup>.



**Figure 14.** The impact of nitrogen flow rate on product efficiency at 600 °C temperature and 100 °C.min<sup>-1</sup> heating rate.



**Figure 15.** The impact of nitrogen flow rate on product efficiency at 750 °C and 100 °C.min<sup>-1</sup>.

The highest value in Figure 11 is 57.9 wt% at 300 cm<sup>3</sup>.min<sup>-1</sup>, while the lowest is 47.84 wt% at 50 cm<sup>3</sup>.min<sup>-1</sup> at 300 °C and 100 °C.min<sup>-1</sup>. It has been found that the nitrogen flow rate has less impact on pyrolysis conversion at middle speeds (100–200 cm<sup>3</sup>.min<sup>-1</sup>).

In contrast, pyrolysis conversion increases to its highest value at  $300 \text{ cm}^3 \cdot \text{min}^{-1}$  due to increased gas product yield. Once more, when Figure 11 is reviewed, it is clear that the highest liquid product yield value is 41.8 wt% at a nitrogen flow rate of  $100 \text{ cm}^3 \cdot \text{min}^{-1}$ , and the lowest value is 29.52 wt% at  $300 \text{ cm}^3 \cdot \text{min}^{-1}$ . It is thought that the rise in the gas product yield caused the reduction in the liquid product yield with the increase at  $300 \text{ cm}^3 \cdot \text{min}^{-1}$ . The maximum value in solid product yield is 52.16 wt% at  $50 \text{ cm}^3 \cdot \text{min}^{-1}$ , while the lowest value is 42.06 wt% at a  $300 \text{ cm}^3 \cdot \text{min}^{-1}$ . When comparing the change in gas production, it can be noted that the best efficiency is 28.42 wt% at  $300 \text{ cm}^3 \cdot \text{min}^{-1}$ , and the lowest efficiency is 8.82 wt% at  $100 \text{ cm}^3 \cdot \text{min}^{-1}$ . It is also determined, based on the data shown in Figure 11, that the decline in the efficiency of the liquid and solid is responsible for the rise in the gas product yield at  $300 \text{ cm}^3 \cdot \text{min}^{-1}$ .

Figure 12 shows that at  $100 \text{ }^\circ\text{C} \cdot \text{min}^{-1}$  and  $400 \text{ }^\circ\text{C}$ , the best pyrolysis conversion value is 78.49 wt% at  $300 \text{ cm}^3 \cdot \text{min}^{-1}$ , and the lowest value is 69.82 wt% at  $50 \text{ cm}^3 \cdot \text{min}^{-1}$ . The efficiency of producing liquid products ranges from 46.41 wt% at  $50 \text{ cm}^3 \cdot \text{min}^{-1}$  to 50.5 wt% at  $300 \text{ cm}^3 \cdot \text{min}^{-1}$ . Considering the effect of nitrogen flow rate on solid product yield, it is seen that the highest yield value is 30.18 wt% at  $100 \text{ cm}^3 \cdot \text{min}^{-1}$ , and the lowest yield value is 21.52 wt% at  $300 \text{ cm}^3 \cdot \text{min}^{-1}$ . The efficiency is observed between 23.41 wt% at a nitrogen flow rate of  $50 \text{ cm}^3 \cdot \text{min}^{-1}$  to 27.99 wt% at  $300 \text{ cm}^3 \cdot \text{min}^{-1}$  for producing gas products. The maximum pyrolysis conversion efficiency is 81.84 wt% at  $300 \text{ cm}^3 \cdot \text{min}^{-1}$ , while the lowest efficiency is 78.73 wt% at  $50 \text{ cm}^3 \cdot \text{min}^{-1}$ , according to Figure 13. This is at a  $500 \text{ }^\circ\text{C}$  fast pyrolysis temperature and a  $100 \text{ }^\circ\text{C} \cdot \text{min}^{-1}$  heating rate. The greatest value for liquid product efficiency is 69.77 wt% at  $50 \text{ cm}^3 \cdot \text{min}^{-1}$ , whereas the lowest value is 58.24 wt% at  $100 \text{ cm}^3 \cdot \text{min}^{-1}$ .

When considering how nitrogen flow rate affects solid product output, it can be noted that the greatest value is 21.27 wt% at a nitrogen flow rate of  $50 \text{ cm}^3 \cdot \text{min}^{-1}$ , and the lowest value is 18.16 wt% at  $300 \text{ cm}^3 \cdot \text{min}^{-1}$ . It can be seen that the gas product yield is shown between 8.96 wt% at  $50 \text{ cm}^3 \cdot \text{min}^{-1}$  nitrogen flow rate to 23.38 wt% at  $100 \text{ cm}^3 \cdot \text{min}^{-1}$ . In Figure 14, the greatest value in the pyrolysis conversion is 82.28 wt% at  $50 \text{ cm}^3 \cdot \text{min}^{-1}$ , and the lowest value is 78.23 wt% at  $200 \text{ cm}^3 \cdot \text{min}^{-1}$ . This is at a  $600 \text{ }^\circ\text{C}$  pyrolysis temperature and a  $100 \text{ }^\circ\text{C} \cdot \text{min}^{-1}$  heating temperature. The greatest value for liquid product efficiency is 57.51 wt% at  $100 \text{ cm}^3 \cdot \text{min}^{-1}$ , while the lowest value is discovered to be 47.83 wt% at  $200 \text{ cm}^3 \cdot \text{min}^{-1}$ . The greatest value is 21.77 wt% at  $200 \text{ cm}^3 \cdot \text{min}^{-1}$ , and the lowest is 17.72 wt% at  $50 \text{ cm}^3 \cdot \text{min}^{-1}$ , following the research on the impact of nitrogen flow rate on solid product output. It can be noticed that the gas product yield ranges from 21.02 wt% at  $100 \text{ cm}^3 \cdot \text{min}^{-1}$  to 30.4 wt% at  $200 \text{ cm}^3 \cdot \text{min}^{-1}$ . When Figure 15 is inspected, it can be observed that the maximum pyrolysis conversion efficiency is 85.14 wt% at  $300 \text{ cm}^3 \cdot \text{min}^{-1}$ , and the lowest efficiency is 79.07 wt% at  $100 \text{ cm}^3 \cdot \text{min}^{-1}$ . This is at  $750 \text{ }^\circ\text{C}$  and a  $100 \text{ }^\circ\text{C} \cdot \text{min}^{-1}$  heating rate. A nitrogen flow rate of  $300 \text{ cm}^3 \cdot \text{min}^{-1}$  produces the best liquid efficiency, while a nitrogen flow rate of  $200 \text{ cm}^3 \cdot \text{min}^{-1}$  generates the lowest. The maximum yield is obtained at  $100 \text{ cm}^3 \cdot \text{min}^{-1}$ , and the lowest yield is recorded at  $300 \text{ cm}^3 \cdot \text{min}^{-1}$  when the impact of nitrogen flow rate on solid product efficiency is investigated. A nitrogen flow rate of  $200 \text{ cm}^3 \cdot \text{min}^{-1}$  generates the greatest value in gas product production.

#### 4. Conclusions

The information gained indicates that the current biomass mixture possesses the qualities necessary for biomass samples that may be used to produce biofuels, considering the findings of a proximate analysis and the heating value of the biomass mixture utilized in the pyrolysis tests. After the proximate analysis procedures and the calorific value of the combination are determined, the heating value of the bio-oil acquired from the fast pyrolysis experiments under the most efficient circumstances ( $50 \text{ cm}^3 \cdot \text{min}^{-1}$ ,  $500 \text{ }^\circ\text{C}$ ,  $100 \text{ }^\circ\text{C} \cdot \text{min}^{-1}$ ) is 5900 cal/gr. When the heating value of the raw material mixture is compared with the heating value of the bio-oil obtained as a result of fast pyrolysis, it is seen that the heating value of the raw bio-oil is practically 39.91% higher than the raw material mixture. This increment in energy content is suitable for converting biomass directly used as fuel into



liquid products with a higher energy content by fast pyrolysis. The solid product yield is typically high in this study's experiments conducted between 300 and 400 °C; the liquid product yield generally rises at 500 and 600 °C, which are considered medium temperatures for fast pyrolysis, and at high temperatures (600–750 °C). The influence of the solid and gas product yields reduces the liquid product yield. It is established in this investigation that the pyrolysis temperature of 500 °C produced the maximum liquid product yield value of 69.77 wt%. Coking at a low temperature and high heating rate increased solid product efficiency while decreasing liquid and gas product yields in studies examining the influence of heating rate on product yields. It has been determined that 100 °C.min<sup>-1</sup> is the optimum heating rate for the liquid yield. According to the results acquired, in Figure 10, it is noted that the liquid yield decreases due to the increase in gas yield at very high heating rates (400–600 °C.min<sup>-1</sup>) and the increase in solid yield due to coking. The value of 15.80 wt% obtained as the lowest solid product yield at a heating rate of 400 °C.min<sup>-1</sup> and a temperature of 300 °C indicates this situation. It is discovered through the fast pyrolysis carried out in this research that the liquid yield is at its highest at 500 °C and 50 cm<sup>3</sup>.min<sup>-1</sup>.

This is likely because condensable gases leave the refrigerant more quickly, and the gases produced during pyrolysis are swiftly entrained when the nitrogen flow rate for entraining is high. Due to this, when the flow rate is increased from 50 to 300 cm<sup>3</sup>.min<sup>-1</sup>, a general increase in the yield of non-condensable gases and a general decrease in the yield of liquid products are seen.

A biomass power plant generates energy using the steam produced while burning plant or animal materials in a combustion chamber. This procedure is carried out in various steps. In a combustion chamber, the biomass is burned.

The biomass produces heat, which warms water in a boiler. The water is converted into steam, which is then pushed through turbines. The steam turns into a turbine, which powers an alternator. The alternator generates alternating electric current using the energy supplied by the turbine. A transformer enhances the voltage of the electric current produced by the alternator, allowing it to be transmitted more readily on medium and high-voltage lines. Some of the steam is collected and reused at the turbine's outlet for heating. The liquid product for mixing with diesel fuel in diesel engines and biomass plants contains a very high potential. As it is known, bio-oil is used in diesel engines by mixing it with diesel fuels. The heat release profiles of bio-oils mixed with diesel fuel are consistent with slow burning chemistry and fast mixing compared to diesel fuel; longer ignition delays of bio-oils are due to slow chemistry compared to diesel fuel, and as a result, diesel combustion is mainly limited to the mixing ratio. At the same time, the combustion of pyrolysis oil indicates that the process is mainly limited by its chemical structure. Considering the industrial applications mentioned above, if the potential of the current study is evaluated, Turkey can be considered quite rich regarding raw material waste resources used in this study. Turkey ranks fourth in walnut production after China, the USA, and Iran, with its output approaching 300,000 tons. In addition, when the current situation for the tea bush, which is another raw material used, is evaluated, as of 2022, 791,287 decares of tea area are pruned with the 1/7 pruning law every year, which constitutes a substantial potential in terms of biomass waste potential. Considering that the highest liquid product yield of this pyrolysis study was 69.77% by weight, it can be thought that approximately 70% of this biomass potential can be converted into a liquid product.

Considering the availability and amount of the biomass raw materials used, the efficiency of the obtained liquid product, and the calorific value of the obtained bio-oil, the existing biomass mixture can be used as a renewable energy source. In particular, the exceptionally high efficiency of the raw bio-oil obtained is an essential advantage in obtaining liquid fuel from biomass. In addition, the thermal value of the produced raw bio-oil is relatively high compared to its raw material and can be considered one of the beneficial results of this study in terms of energy efficiency.

**Author Contributions:** Conceptualization, M.Ş.G.; Methodology, T.K., Ö.K., S.S., J.M.O. and J.-S.H.; Software, T.K. and J.M.O.; Validation, T.K., Ö.K., M.Ş.G., S.K. and S.S.; Formal analysis, T.K., Ö.K., S.K. and A.B.O.; Investigation, T.K., M.Ş.G., E.C. and S.S.; Resources, Ö.K., M.Ş.G., E.C., S.S., J.M.O. and J.-S.H.; Data curation, E.C., S.K., B.E.K.N. and J.-S.H.; Writing—original draft, Ö.K., M.Ş.G., E.C., S.K. and A.B.O.; Writing—review & editing, T.K., Ö.K., E.C., S.S. and A.B.O.; Visualization, M.Ş.G.; Supervision, J.-S.H.; Project administration, A.B.O., B.E.K.N. and J.-S.H.; Funding acquisition, A.B.O., B.E.K.N. and J.-S.H. All authors have read and agreed to the published version of the manuscript.

**Funding:** This work was supported by the National Research Foundation of Korea (NRF), a grant funded by the Korean government Ministry of Science and ICT (MSIT) (No. NRF-2021R1A5A8033165); the Korea Institute of Energy Technology Evaluation and Planning (KETEP) and the Ministry of Trade, Industry & Energy (MOTIE) of the Republic of Korea (No. 2022400000150).

**Data Availability Statement:** The article data is not archived anywhere and all study data can be seen in the article.

**Conflicts of Interest:** The authors declare no conflict of interest.

## References

- Zizic, M.C.; Mladineo, M.; Gjeldum, N.; Celent, L. From Industry 4.0 towards Industry 5.0: A Review and Analysis of Paradigm Shift for the People, Organization and Technology. *Energies* **2022**, *15*, 5221. [CrossRef]
- Gielen, D.; Boshell, F.; Saygin, D.; Bazilian, M.D.; Wagner, N.; Gorini, R. The role of renewable energy in the global energy transformation. *Energy Strategy Rev.* **2019**, *24*, 38–50. [CrossRef]
- Bahadır, A.; Kar, T.; Keleş, S.; Kaygusuz, K. Bio-oil production from fast pyrolysis of maple fruit (*acer platanoides samaras*) product yields. *World J. Eng.* **2019**, *14*, 55–59. [CrossRef]
- Kar, T.; Keleş, S. Characterisation of bio-oil and its sub-fractions from catalytic fast pyrolysis of biomass mixture. *Waste Manag. Res.* **2019**, *37*, 674–685. [CrossRef] [PubMed]
- Kalak, T. Potential Use of Industrial Biomass Waste as a Sustainable Energy Source in the Future. *Energies* **2023**, *16*, 1783. [CrossRef]
- Lamb, W.F.; Wiedmann, T.; Pongratz, J.; Andrew, R.; Crippa, M.; Olivier, J.G.J.; Wiedenhofer, D.; Mattioli, G.; Al Khourdajie, A.; House, J.; et al. A review of trends and drivers of greenhouse gas emissions by sector from 1990 to 2018. *Environ. Res. Lett.* **2021**, *16*, 073005. [CrossRef]
- Andrew, J.J.; Dhakal, H. Sustainable biobased composites for advanced applications: Recent trends and future opportunities—A critical review. *Compos. Part C Open Access* **2022**, *7*, 100220. [CrossRef]
- The United Nations Environment Programme. Annual Report (UNEP). 2022. Available online: [https://wedocs.unep.org/bitstream/handle/20.500.11822/41679/Annual\\_Report\\_2022.pdf?sequence=3](https://wedocs.unep.org/bitstream/handle/20.500.11822/41679/Annual_Report_2022.pdf?sequence=3) (accessed on 4 September 2023).
- Republic of Turkey Ministry of Energy and Natural Resources (ETKB). Turkey Biomass Energy Potential Atlas (BEPA). 2022. Available online: <https://bepa.enerji.gov.tr/> (accessed on 4 September 2023).
- Antar, M.; Lyu, D.; Nazari, M.; Shah, A.; Zhou, X.; Smith, D.L. Biomass for a sustainable bioeconomy: An overview of world biomass production and utilization. *Renew. Sustain. Energy Rev.* **2021**, *139*, 110691. [CrossRef]
- Mawusi, S.K.; Shrestha, P.; Xue, C.; Liu, G. A comprehensive review of the production, adoption and sustained use of biomass pellets in Ghana. *Heliyon* **2023**, *9*, e16416. [CrossRef]
- Abdoulmoumine, N.; Adhikari, S.; Kulkarni, A.; Chattanathan, S. A review on biomass gasification syngas cleanup. *Appl. Energy* **2015**, *155*, 294–307. [CrossRef]
- Açıklalın, K.; Karaca, F. Fixed-bed pyrolysis of walnut shell: Parameter effects on yields and characterization of products. *J. Anal. Appl. Pyrolysis* **2017**, *125*, 234–242. [CrossRef]
- Osman, A.I.; Farghali, M.; Ihara, I.; Elgarahy, A.M.; Ayyad, A.; Mehta, N.; Ng, K.H.; El-Monaem, E.M.A.; Eltaweil, A.S.; Hosny, M.; et al. Materials, fuels, upgrading, economy, and life cycle assessment of the pyrolysis of algal and lignocellulosic biomass: A review. *Environ. Chem. Lett.* **2023**, *21*, 1419–1476. [CrossRef]
- Mohan, D.; Pittman, C.U., Jr.; Steele, P.H. Pyrolysis of Wood/Biomass for Bio-oil: A Critical Review. *Energy Fuels* **2006**, *20*, 848–889. [CrossRef]
- Cantrell, K.B.; Hunt, P.G.; Uchimiya, M.; Novak, J.M.; Ro, K.S. Impact of pyrolysis temperature and manure source on physico-chemical characteristics of biochar. *Bioresour. Technol.* **2012**, *107*, 419–428. [CrossRef]
- Qin, F.; Zhang, C.; Zeng, G.; Huang, D.; Tan, X.; Duan, A. Lignocellulosic biomass carbonization for biochar production and characterization of biochar reactivity. *Renew. Sustain. Energy Rev.* **2022**, *157*, 112056. [CrossRef]
- Kar, T.; Keleş, S.; Kaygusuz, K. Comparison of catalytic and noncatalytic pyrolysis and product yields of some waste biomass species. *Int. J. Energy Res.* **2019**, *43*, 2032–2043. [CrossRef]
- Debdoubi, A.; El Amarti, A.; Colacio, E.; Blesa, M.J.; Hajjaj, L.H. The effect of heating rate on yields and compositions of oil products from esparto pyrolysis. *Int. J. Energy Res.* **2006**, *30*, 1243–1250. [CrossRef]

20. Akhtar, J.; Amin, N.S. A review on operating parameters for optimum liquid oil yield in biomass pyrolysis. *Renew. Sustain. Energy Rev.* **2012**, *16*, 5101–5109. [[CrossRef](#)]
21. Parthasarathy, P.; Al-Ansari, T.; Mackey, H.R.; McKay, G. Effect of heating rate on the pyrolysis of camel manure. *Biomass Convers. Biorefinery* **2023**, *13*, 6023–6035. [[CrossRef](#)]
22. Wang, B.; Xu, F.; Zong, P.; Zhang, J.; Tian, Y.; Qiao, Y. Effects of heating rate on fast pyrolysis behavior and product distribution of Jerusalem artichoke stalk by using TG-FTIR and Py-GC/MS. *Renew. Energy* **2019**, *132*, 486–496. [[CrossRef](#)]
23. Hu, Q.; Cheng, W.; Mao, Q.; Hu, J.; Yang, H.; Chen, H. Study on the physicochemical structure and gasification reactivity of chars from pyrolysis of biomass pellets under different heating rates. *Fuel* **2022**, *314*, 122789. [[CrossRef](#)]
24. Fu, J.; Liu, J.; Xu, W.; Chen, Z.; Evrendilek, F.; Sun, S. Torrefaction, temperature, and heating rate dependencies of pyrolysis of coffee grounds: Its performances, bio-oils, and emissions. *Bioresour. Technol.* **2022**, *345*, 126346. [[CrossRef](#)] [[PubMed](#)]
25. El-Sayed, S.A.; Khairy, M. Effect of heating rate on the chemical kinetics of different biomass pyrolysis materials. *Biofuels* **2015**, *6*, 157–170. [[CrossRef](#)]
26. Wu, Y.; Wang, K.; Wei, B.; Yang, H.; Jin, L.; Hu, H. Pyrolysis behavior of low-density polyethylene over HZSM-5 via rapid infrared heating. *Sci. Total Environ.* **2022**, *806*, 151287. [[CrossRef](#)]
27. Food and Agriculture Organization of the United Nations FAO. Walnuts Production Statistics. 2022. Available online: <http://www.fao.org/faostat/en/#data/QC> (accessed on 4 September 2023).
28. General Directorate of Turkish Tea Businesses (ÇAYKUR). Annual Report. 2022. Available online: <https://www.caykur.gov.tr/Pages/Yayinlar/YayinDetay.aspx?ItemType=2&ItemId=941> (accessed on 4 September 2023).
29. General Directorate of Forestry of Türkiye, Türkiye's Forestry Assesses OGM. 2020. Available online: <https://www.ogm.gov.tr/tr/ormanlarimizsitesi/TurkiyeOrmanVarligi/Yayinlar/2020%20T%C3%BCrkiye%20Orman%20Varl%C4%B1%C4%9F%C4%B1.pdf> (accessed on 4 September 2023).
30. Li, J.; Yan, R.; Xiao, B.; Wang, X.; Yang, H. Influence of temperature on the formation of oil from pyrolyzing palmoil wastes in a fixed bed reactor. *Energy Fuels* **2007**, *21*, 2398–2407. [[CrossRef](#)]
31. Ateş, F.; Işıkdag, M.A. Evaluation of the role of the pyrolysis temperature in straw biomass samples and characterization of the oils by GUMS. *Energy Fuels* **2008**, *22*, 1936–1943. [[CrossRef](#)]
32. Hanif, M.U.; Capareda, S.C.; Iqbal, H.; Arazo, R.O.; Baig, M.A. Effects of Pyrolysis Temperature on Product Yields and Energy Recovery from Co-Feeding of Cotton Gin Trash, Cow Manure, and Microalgae: A Simulation Study. *PLoS ONE* **2016**, *11*, e0152230. [[CrossRef](#)]
33. Pütün, E. Catalytic pyrolysis of biomass: Effects of pyrolysis temperature, sweeping gas flow rate and MgO catalyst. *Energy* **2010**, *35*, 2761–2766. [[CrossRef](#)]
34. Kan, T.; Strezov, V.; Evans, T.J. Lignocellulosic biomass pyrolysis: A review of product properties and effects of pyrolysis parameters. *Renew. Sustain. Energy Rev.* **2016**, *57*, 1126–1140. [[CrossRef](#)]
35. Williams, P.T.; Besler, S. The influence of temperature and heating rate on the slow pyrolysis of biomass. *Renew. Energy* **1996**, *7*, 233–250. [[CrossRef](#)]
36. Niu, Y.; Tan, H.; Liu, Y.; Wang, X.; Xu, T. The Effect of Particle Size and Heating Rate on Pyrolysis of Waste Capsicum Stalks Biomass. *Energy Sources Part A Recover. Util. Environ. Eff.* **2013**, *35*, 1663–1669. [[CrossRef](#)]
37. Onay, O. Influence of pyrolysis temperature and heating rate on the production of bio-oil and char from safflower seed by pyrolysis, using a well-swept fixed-bed reactor. *Fuel Process. Technol.* **2007**, *88*, 523–531. [[CrossRef](#)]
38. Keleş, S.; Kar, T.; Akgün, M.; Kaygusuz, K. Catalytic fast pyrolysis of hazelnut cupula: Characterization of bio-oil. *Energy Sources Part A Recover. Util. Environ. Eff.* **2017**, *39*, 2216–2225. [[CrossRef](#)]

**Disclaimer/Publisher's Note:** The statements, opinions and data contained in all publications are solely those of the individual author(s) and contributor(s) and not of MDPI and/or the editor(s). MDPI and/or the editor(s) disclaim responsibility for any injury to people or property resulting from any ideas, methods, instructions or products referred to in the content.